The Potency of *Camellia Sinensis* L. to Reduce Proinflammatory Cytokine Levels in the Acute Respiratory Distress Syndrome Rat Model

Wahyu Widowati[1,*], Didik Priyandoko[2], Hanna Sari Widya Kusuma[3], Rizal Rizal[3,4]

[1]Faculty of Medicine, Maranatha Christian University, Jalan Surya Sumantri No. 65, Bandung 40164, Indonesia
[2]Faculty of Mathematics and Natural Science Education, Universitas Pendidikan Indonesia, Jalan Dr. Setiabudi No. 229, Bandung 40154, Indonesia
[3]Biomolecular and Biomedical Research Center, Jalan Babakan Jeruk II No. 9, Bandung 40163, Indonesia
[4]Biomedical Engineering Department of Electrical Engineering, Faculty of Engineering, University of Indonesia, Jalan Prof. DR. Ir R. Roosseno, Beji, Depok 16425 Indonesia
*Email: wahyu_w60@yahoo.com

Abstract. This study was conducted in order to ascertain how green tea extract (GTE) could affect inflammatory markers, including level of interleukin-(IL)-12, IL-18 of serum and lung, tumor necrosis factor (TNF)-α, gene expression of NLR family-pyrin-domain containing 3 (NLRP3) of lung, nuclear factor kappa B (NF-κB), lung histopathology, and IL-6 expression of lung tissue in lipopolysaccharide (LPS)-treated rats as ARDS animal model. Rats were given GTE at dosages of 0, 50, 400, 800 mg/kg of body weight for 28 days to boost their immune systems. The rats were then stimulated with LPS (5 g/kg of BW) and after that continued to receive GTE for 28 days. Levels of serum or lung IL-18, IL-12, TNF-α, were measured using the ELISA method; expression of lung NF-κB and NLRP3 was measured by qRT-PCR; immunohistochemistry (IHC) was implemented to assess lung IL-6 expression; and lung histopathology was evaluated through the bleeding, inflammation, and alveolus scores. GTE had the ability to lower serum IL-18, lung TNF-α, and lung IL-12 levels; suppress the lung gene expression of NF-κB, NLRP-3, IL-6 expression; and improve lung histopathology. Green tea extract inhibited inflammation in the ARDS rat model by decreasing the proinflammatory cytokine level and proinflammatory gene expression.

Keywords: *acute respiratory distress syndrome; Camellia sinensis; COVID-19; inflammation; lung.*

1   Introduction

The stability of the healthcare systems all over the world has been hampered because of the surfacing of the SARS-CoV-2 coronavirus [1]. Alarming acute respiratory distress syndrome (ARDS) outcomes in COVID-19 patients have

been associated with a large increase in cytokine production or cytokine storm [2,3]. During the early infection stage, a delayed release of cytokines and chemokines as well as a low-level release of interferons (IFNs) occurs, and an enormous amount of inflammatory cells invade the lung tissue quickly, releasing pro-inflammatory cytokines and chemokines to attract them, which causes damage [2,3]. Thus, it is claimed that lung disease may be caused by inflammatory cells.

During the inflammatory process, a variety of immune cells generate pro-inflammatory cytokines and enzymes that inhibit inflammation, namely interleukin-1 (IL-1), interleukin-4 (IL-4), tumor necrosis factor (TNF)-α, matrix metalloproteinases (MMPs), and cyclooxygenases (COXs) [4]. Nevertheless, unregulated acute inflammation can transition into a chronic state, thereby contributing to the development of specific chronic inflammatory conditions [5]. In this study, IL-6, IL-18, IL-12, NF-κB, NLRP3, and TNF-α (NLR family pyrin domain containing 3) were selected as interrelated pro-inflammatory markers. The NLRP3 inflammasome, comprising a combination of various proteins, promotes lung inflammation in the context of SARS-CoV-2 infection [6]. The growth of numerous inflammatory illnesses is linked to the activation and aberrant regulation of NLRP-3 inflammasome. By attaching to toll-like receptors (TLRs), lipopolysaccharide (LPS) can cause the potential to activate NLRP-3 expression. The initiation of the NLRP3 inflammasome leads to the liberation of IL-1 and IL-18, potentially leading to pyroptosis, a type of programmed cell demise [6]. In the context of innate immunity, the production of pro-inflammatory cytokines is facilitated by the activity of the nuclear factor kappa-light-chain-enhancer of activated B (NF-κB). IL-18 is an inflammatory cytokine relevant to inflammatory signaling pathways; both can regulate the inflammatory response. NF-kB can be triggered by NLRP3, and an active NF-kB can increase the transcription of inflammatory factor genes [7]. Alveolar capillary barrier damage causes a life-threatening syndrome known as acute lung inflammation and elevated pulmonary permeability, defined as ARDS [8]. ARDS is caused by a variety of risk factors, including pulmonary infection along with extra-pulmonary factors including infection, trauma, large blood transfusion, drowning, drug overdose, fat embolism, and breathing poisonous gases [9]. The recent COVID-19 pandemic resulted in a large number of severe ARDS cases, which had a global impact on the health sector. This has led to the study of various plant-based products for potential therapeutic application due to the need for new therapeutics in the field of lung inflammatory diseases.

Polyphenols are one of the most promising natural compounds for treating chronic inflammation. Tea (*Camellia sinensis* L.) contains a lot of polyphenols, which reportedly possess anti-inflammatory qualities by preventing the creation and activation of different pro-inflammatory mediators [10]. Recent research in

the fields of science and medicine has revealed that green tea has a number of pharmacological and toxicological effects on both people and animals, including anti-inflammatory characteristics [11].

A crucial element within the gram-negative bacteria's cell walls is lipopolysccharide (LPS). Since practically all gram-negative bacteria share it, it is a highly conserved and powerful inflammatory inducer [12]. LPS-induced lung damage is among the most popular rat ARDS models and was designed in order to replicate the neutrophilic inflammatory response found in ARDS [13]. This study aims to investigate green tea extract (GTE) anti-inflammatory activities, including TNF-α from the lungs, IL-12, IL-18 levels in blood and IL-6 protein expression of lung, the expression of lung NF-kB and NLRP-3, and the lung histology in rats exposed to LPS.

2   Research Methods

2.1   Chemicals

GTE was obtained from PT. Fathonah Amanah Shidiq Tabligh (Depok, Indonesia) (Batch no. 00107201057). *Escherichia coli* O55:B5-derived lipopolysaccharide was obtained from Sigma-Aldrich Inc. in St. Louis, Missouri, USA (L2630-25MG). ELISA Kits of TNF-α (E-EL-R0019), IL-12 (E-EL-R0064), IL-18 (E-EL-R0567), and IL-6 polyclonal antibody (E-AB-40073) were purchased from Elabscience, Houston, TX, USA. A Rabbit Specific HRP/DAB (ABC) Detection IHC Kit was acquired from Abcam (ab64261). Hydrogen peroxide (H_2O_2) (1072091000) and methanol (1060092500) were purchased from Merck. A SsoFast Evagreen Supermix Kit for quantitative PCR (qPCR) and an iScript Reverse Transcription Supermix Kit for RT-PCR (Bio-Rad, 170-8841) were purchased from Bio-Rad Laboratories, Hercules, USA. TRI reagent and Direct-zol RNA Miniprep Plus for RNA purification were procured from Zymo Research, Irvine, CA, USA (R2072). Ketamine (Ikapharmindo Putramas) and xylazine (361453, Interchemie) were used as rat anesthetic. In this work, only analytical-grade chemical reagents were employed.

2.2   Green Tea Extract Preparation

Ethanol 70% solvent was employed on green tea leaves, resulting in the production of green tea extract (GTE) by PT Fathonah Amanah Shidiq Tabligh (Depok, Indonesia) (Batch no. 00107201057), following the Good Manufacturing Practice (GMP) standards of the Indonesian Food and Drug Authority (BPOM). GTE was added by lactose, stored at 25±2 °C [14].

2.3   Animals and Experimental Design

At 8 weeks old, 25 male white Sprague Dawley rats (SD) ranging in weight from 150 to 200 g were acquired from IratCo Veterinary Laboratory Services in Bogor. Individually ventilated cages (IVC) were used to maintain them with the temperature set at a range of 20 °C to 24 °C under 12-hours of light from 06:00 to 18:00, followed by 12 hours of darkness. Throughout the process, the surrounding humidity level remained steady. Throughout the examinations, 14% protein and 5% fat meals were given to all animals on an as-needed basis. After one week of habituation, GTE was administered to the rats for the first 28 days at dosages of 50, 400, and 800 mg/kg BW [15,17]. Furthermore, the rats in the positive group were intra-tracheally induced once with LPS at 5 mg/kg BW. The rats were further administered GTE for 28 days. Five groups of five rats each were randomly assigned in this study: rats that were not treated (the negative control), rats that received intratracheal LPS at a dose of 5 mg/kg BW (positive control, PC), and rats where the PC group received 0, 50, 400, and 800 mg GTE/kg BW every day (for 28 days). The LPS-induced rats began to exhibit ARDS symptoms such as nasal discharge and sneezing after 8 hours. The rats were then put to death after 28 days with an intraperitonial shot of xylazine (15 mg/kg BW) and ketamine (100 mg/kg BW). The right lung was then removed and stored in liquid nitrogen right away, after which it was maintained at -80 °C until needed. The left lung was saved for dissection for hematoxylin and eosin (HE) and immunohistochemistry (IHC) analysis [18,19].

2.4   Ethical Statement

The animal experiment was carried out under a protocol accepted by the Maranatha Christian University (Faculty of Medicine), Bandung, Indonesia (no. 099/KEP/VII/2020).

2.5   Measurement of Serum IL-18, Lung TNF-α, and IL-12

Rat serum was quantified for IL-18 using an ELISA kit, and the frozen lungs of the rats were homogenized and measured for TNF-α, IL-12, and IL-18. The steps were followed exactly as instructed by the manufacturer. A microplate reader (Multiskan GO, Thermo Scientific) was employed to measure the absorbance of the samples at 450 nm. The protein standard-curve was employed to compute the IL-18, TNF- α, and IL-12 levels [20,21].

2.6   HE Analysis

Regular processing was done on the lung tissues that had been fixed in formalin 10%, including paraffin embedding, sectioning, deparaffinizing, and rehydrating [22]. Standard methods were used to examine the morphological alterations in

the HE-stained sections of the lung tissues, and OriginPro 8.5 was used to estimate the alveolus, inflammation, and bleeding scores [23].

2.7 Semiquantification Immunohistochemistry of IL-6

IHC staining and antigen retrieval were executed in a citrate buffer with pH 6.0 in 10 minutes at 121 °C. Methanol and 3% H_2O_2 were used to block endogenous peroxidase for 15 minutes at ambient temperature. At normal temperature, the main Rabbit Anti-Rat IL-6 was incubated for the whole night. Then, utilizing the Rabbit Specific HRP/DAB (ABC) Detection IHC-Kit, the target proteins were seen. It was HE that was used as a counterstain. A Primostar (Zeiss) microscope was used to view the stained tissues, and photos were taken using a Lumenera Infinity 1-3c. This field of view was taken five times in different areas on one slide, determined from the area that represents the overall result, the average color thickness, or by looking at where the target protein is expressed. The ImageJ software was used to assess the positive cell index on the IHC slides as a semi quantification method expressed as a percent of area per total area [18,22-25].

2.8 Quantification of NF-κB and NLRP-3 Gene Expression by qRT-PCR

In line with the guidelines provided by the manufacturer, the Direct-zol RNA Miniprep Plus Kit was used to extract and purify the total RNA from the rat's lungs. In Table 1, the primer sequences are displayed. Utilizing the iScript Reverse Transcription-Supermix Kit for-RT-PCR, complementary DNA was created by reverse-transcribing 15 µL of RNA into single-stranded DNA (cDNA) in a two-step RT-PCR process. At 260/280 nm, each sample's RNA concentration and purity were determined, as shown in Table 2. The AriaMx-3000 Real-Time PCR System was used to measure gene expression quantitatively. The PCR process included an initial pre-incubation cycle at 95°C for five minutes, followed by 40 cycles consisting of denaturation at 95°C for 1 minute, annealing at 57°C for 40 seconds, and extension at 72°C for 1 minute. The qRT-PCR reaction mixture was prepared using the Evagreen master mix [18,20,21,23,26].

The gene level expression was calculated with the following equation [27]:

$$\Delta\Delta Cq = (\Delta Cq\ treated - \Delta Cq\ control)$$

$$\text{Gene level expression} = \left(2^{\Delta\Delta Cq}\right)$$

Table 1 Sequences of primers for NF-κB, NLRP3, and GAPDH genes.

Gene symbols	Primer sequence (5' to 3') upper strand: sense lower strand: anti-sense	Product size (bp)	Annealing (°C)	Cycle	References
Rat NF-κB	5'-GGACTATGACTTGAATGCGG-3' 5'-ACACCTCAATGTCTTCTTTCTG-3'	230	57	40	NCBI Reference Sequence: NM_199267.2
Rat NLRP-3	5'-CAGATGCTGGAGTTAGACAACTG-3' 5'-TTCAGAACCTCACAGAGCGT-3'	153	57	40	NCBI Reference Sequence: NM_001191642.1
Rat GAPDH	5'-TCAAGATGGTGAAGCAG-3' 5'-ATGTAGGCCATGAGGTCCAC-3'	217	57	40	NCBI Reference Sequence: NM_001289726

Table 2 Purity and concentration of RNA.

Treatment	RNA concentration (ng/ml)	RNA purity ($\lambda260/\lambda280$ nm)
Negative control (NC)	228.64	2.2636
Positive control (PC)	260.48	2.1947
Positive Control (PC) + GTE 50 mg/kg BW	474.28	1.9809
Positive Control (PC) + GTE 400 mg/kg BW	55.92	1.8881
Positive Control (PC) + GTE 800 mg/kg BW	89.52	2.1131

2.9   Statistical Analysis

The data underwent statistical analysis using SPSS 20.0 software (IBM Corp., Armonk, NY, USA), and the results of the experiments are presented as mean ± SD. One-way analysis of variance, along with Tukey's and Dunnett's post hoc tests, was employed. The comparison between the two groups utilized the HSD. The independent-samples T-Test was run to examine the distinctions among the two groups, with a significance level set at $P \leq 0.05$.

3   Results and Discussion

3.1   Results of the Research

3.1.1   Effect of GTE toward IL-12, TNF-α, and IL-18 Level

TNF-α is a cytokine with pro-inflammatory properties that is known to contribute to LPS-induced lung inflammation. The highest TNF-α level was shown from positive control group and GTE treatment had the ability to decrease the TNF-α level. GTE at 50, 400, and 800 mg/kg of BW effectively reduced TNF-α levels in rats depending on the dosage. A substantial difference between GTE treatment

and positive control at BW 800 mg/kg was observed. The impact of GTE treatment on the level of TNF-α can be seen in Figure 1A.

IL-12 is a cytokine with pro-inflammatory properties that is known to contribute to LPS-induced lung inflammation. The positive control showed the highest IL-12 level and GTE treatment had the ability to decrease the IL-12 level. GTE at 800, 400, and 50 mg/kg of BW was able to reduce the IL-12 level in the rat model depending on the dosage. GTE at 400 and 800 mg/kg of BW revealed a noticeable change from the positive control. GTE at 800 mg/kg-BW suppressed the IL-12 lung level in the ARDS rat model the most. The effect of GTE treatment on IL-12 level can be seen in Figure 1B.

IL-12 is a cytokine with pro-inflammatory properties that is known to contribute to LPS-induced serum inflammation. The positive control showed the highest IL-18 level and GTE treatment had the capacity to lower the amount of IL-18. GTE at 800, 400, and 50 mg/kg of BW showed the capacity to reduce the IL-18 level. GTE at 400 mg/kg of BW decreased the IL-18 level the most significantly. The result of GTE treatment on the IL-18 level is despicable in Figure 1C.
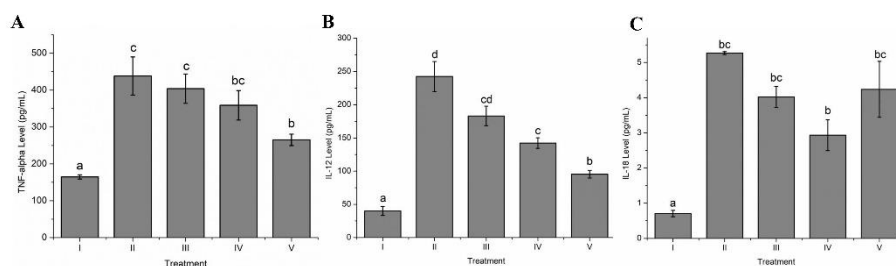

Figure 1 Effect of GTE treatment toward pro-inflammatory cytokine level on ARDS rat model.

A: TNF-α lung level, B: IL-12 lung level, C: IL-18 serum level in ARDS rat model; I: negative-control (NC): untreated rat; II: positive-control (PC): ARDS rat model; III: PC + GTE 50 mg/kg BW; IV: PC + GTE 400 mg/kg BW; V: PC + GTE 800 mg/kg BW. Means ± SD, n = 5. Distinct letters indicate statistically significant variations among various GTE doses based on Tukey's HSD (A) and Dunnett's T3 post hoc-test (B and C) with $P \leq 0.05$.

3.1.2   Effect of GTE Toward HE Analysis

To evaluate the influence of LPS on the lungs in the ARDS model, the lungs were scored for bleeding, inflammation, and alveolus. LPS had the ability to induce lung damage, as well as severe bleeding, moderate inflammation, and severe alveolus. The negative control group, which consisted of normal rats, showed non-specific bleeding, no inflammation, and a normal alveolus.

Based on Figure 2, the negative control, positive control, and GTE treatment groups showed changes in the lungs. Administration of GTE at 50, 400, and 800 mg/kg of BW-improved and decreased the lung damage caused by LPS.

Based on Figures 2 and 3, GTE had the ability to decrease the bleeding score from 3.00 (severe bleeding) to 1.20-1.40 (categorized as mild bleeding). GTE decreased the inflammation score from 2.40 (moderate inflammation) to 1.80 (also categorized as moderate inflammation). GTE also decreased the collapsed alveolus score from 2.80 (severe alveolus) to 1.60-2.13 (moderate alveolus).
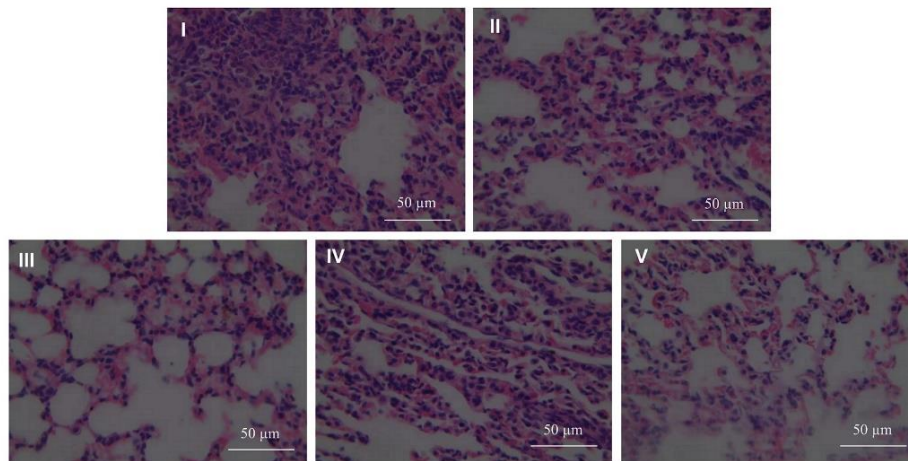

Figure 2 Effect of GTE treatment toward HE analysis on ARDS rat model.

I: negative control (NC): untreated rat; II: positive-control (PC): ARDS rat model; III: PC + GTE 50 mg/kg BW; IV: PC + GTE 400.mg/kg-BW; V: PC + GTE 800 mg/kg-BW.
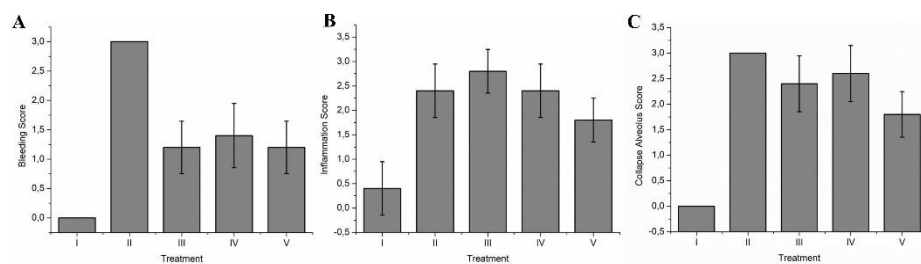

Figure 3 Effect of GTE treatment toward the inflammation, bleeding, and collapsed alveolus score through HE analysis on ARDS rat model.

A: bleeding score; B: inflammation score; C: collapse alveolus score in ARDS rat model. Mean ± SD's, n = 5. I: negative-control (NC): normal rat; II: positive-control (PC): ARDS

rat model; III: PC + GTE of 50 mg/kg of-BW; IV: PC + GTE of 400.mg/kg of-BW; V: PC + GTE of 800.mg/kg of-BW.

3.1.3   Effect of GTE Toward IL-6 Semiquantification by IHC

To evaluate the lungs' inflammation level, they were evaluated using IHC. The NC (normal) group showed a score of 66.60 and the PC group scored 402.60 (Figure 4). Based on Figure 4A, GTE had the ability to decrease IL-6 expression. The most active to decrease the inflammation level was GTE at 800 mg/kg BW.

Based on our observations, a dark brown color indicated damage to the lungs. All GTE treatment groups, except the NC group, had a brown color with different intensities. A dark color indicates specific damage to the lung as a result of LPS induction. The outcomes demonstrated that, in comparison to the PC group, GTE with a dosage of 800 mg/kg BW displayed a brown hue with lower intensity (light brown). Treatment with GTE at 800 mg/kg BW could decrease the expression of IL-6. When comparing the PC group to the other treatment groups, IL-6 expression in this group was the highest. The highest IL-6 expression indicated the most severe damage in cells. Meanwhile, the treatment with GTE showed a lower IL-6 expression relative to the PC group. The lung field-of-view from the IHC analysis is shown in Figure 4B.
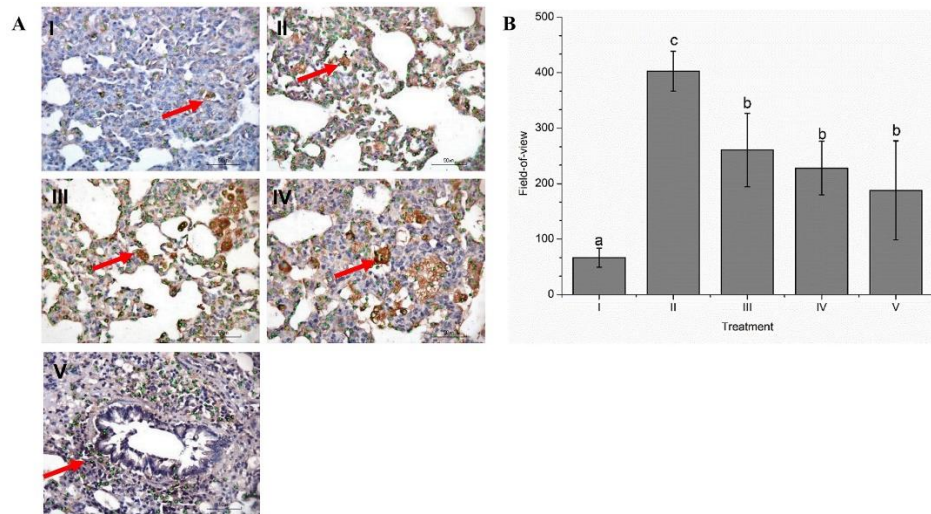

Figure 4 Impact of GTE treatment on the expression of IL-6 in the rat model of ARDS.

A: IL-6 expression by IHC analysis at 50x magnification; B: field-of-view in ARDS rat model. I: negative-control (NC): untreated rat; II: positive-control (PC): ARDS rat model; III: PC + GTE 50 mg/kg BW; IV: PC + GTE 400 mg/kg BW; V: PC+ GTE 800 mg/kg BW. Arrow sign is positive expression of IL-6 in lung of ARDS rat model. Mean ± SD,

n = 3. Distinct letters indicate statistically significant variations among various GTE doses based on Tukey's HSD post hoc test with $P \leq 0.05$.

According to Figure 4B, treatments with GTE decreased the field-of-view toward the PC group. The maximum dosage of GTE (800 mg/kg BW) showed the lowest field-of-view (187.8) compared to GTE 400 mg/kg BW (228) and GTE 50 mg/kg BW (260.60). The decreased field-of-view in the GTE treatment had a significant result towards the PC group.

3.1.4   Effect of GTE toward NF-κB and NLRP3 Gene Expression

Figure 5A showed the impact of GTE treatment toward NF-kB (Figure 5A) and NLRP3 gene expression (Figure 5B). Based on the findings of this investigation, LPS induction in rats could increase NF-κB gene expression. LPS induction could increase NLRP3 gene expression as well.
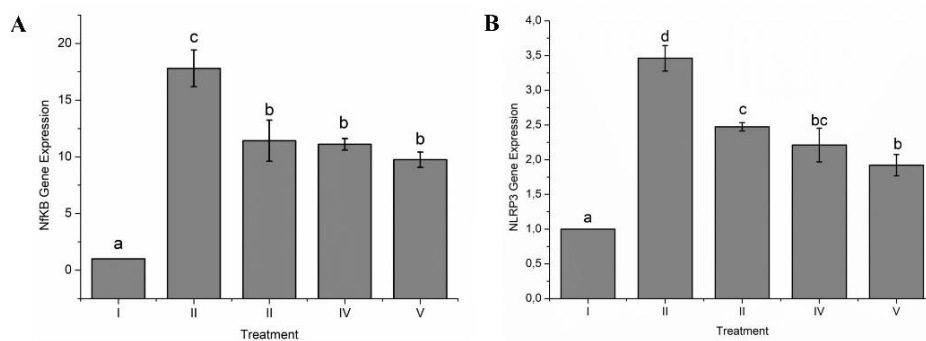

Figure 5 Effect of GTE treatment toward NF-κB and NLRP3 gene expression on the ARDS rat model.

A: NF-κB gene expression; B: NLRP3 gene expression in LPS-induced rats. I: negative-control (NC): untreated-rat; II: positive control (PC): ARDS rat model; III: PC + GTE 50 mg/kg BW; IV: PC + GTE 400 mg/kg BW; V: PC + GTE 800 mg/kg BW. Mean ± SD, n = 5. Distinct letters indicate statistically significant variations among various GTE doses based on Tukey's HSD post hoc test with P ≤ 0.05.

Gene expression of NF-κB was reduced in the GTE treatment groups relative to the positive-control group. The GTE treatment groups had lower expression of the NLRP3 gene in comparison to the positive control. The treatment receiving the highest GTE dosage demonstrated a noteworthy decrease in both NF-κB and NLRP3 gene expression compared to the positive control groups.

3.2   Discussion

The results indicated there was no impact of pretreatment for 28 days prior to LPS induction. The daily measurement of rat body weight remained consistent, and there were no nasal discharges observed. Based on the data (Figure 1-5), LPS could cause ARDS due to inflammatory indicators, such as IL-6, IL-12, IL-18, TNF-α, NF-κB, NLRP-3 and the bleeding, the inflammation, and the collapsed alveolus scores of the damaged lungs. Previous research on ARDS in male Wistar rats induced by LPS inhalation supports these findings [28]. Another study [29] clearly demonstrated that all groups had severe acute injury and a high mortality rate after LPS injection.

LPS causes hemodynamic instability, cardiovascular collapse, and lung damage by inducing unchecked cytokine production. Dysregulation of inflammatory cytokines brought on by LPS is connected with the pathophysiology of depression. LPS causes sepsis, several organ failures, and systemic inflammatory-response syndrome (SIRS). It is also linked with high rates of morbidity and death [30]. These data were validated by a previous study on cytokine-storm-syndrome (CSS) in-COVID-19 patients, together with the inflammatory cytokine levels in the serum, as well as IL-6, IL-1β, IL-2, IL-8, IL-17, IFN-γ-inducible protein 10 (IP10), granulocyte colony-stimulating factor (G-CSF), monocyte chemoattractant protein 1 (MCP1), granulocyte macrophage colony stimulating factor (GM-CSF), macrophage-inflammatory-protein 1α (MIP 1α), and TNF-α were remarkably increased [31]. COVID-19 patients must go through a key step in the NF-κB pro-inflammatory signal pathway [32]. The hyperactivation of the NF-κB transcription factor, which causes ARDS, most likely occurs in non-immune cells like lung epithelial cells [33].

The expression of the NLRP3 gene rises upon the detection of pathogen-associated molecular patterns (PAMPs) like viral RNA and LPS, or damage-associated molecular patterns (DAMPs) like reactive oxygen species (ROS) [34]. When a patient has ARDS, their risk of bleeding and trauma increases, while their blood volume and red blood cell mass and pulmonary-vascular-resistance index (PVRI) levels decrease [35]. The ARDS model's conceptualization comprises alveolar bleeding, severe hypoxemia, edema, and hyaline membrane formation [36]. As a significant clinical issue, ARDS has a high morbidity and fatality rate. The acute stage of ARDS is considered to be characterized histologically by diffuse alveolar damage (DAD). Fibrosis of the alveolar septum, type II pneumocyte hyperplasia, edema, hyaline membranes, and inflammation are all features of the acute phase of DAD [37]. The pathophysiology of ARDS involves edema-flooded airways and unstable alveoli as well as heterogeneous lung collapse. These pathologic alterations lead to alveolar size change [38].

In this study, an elevation in inflammatory indicators was observed, including TNF-α, IL-6, IL-12, and IL-18, attributed to heightened NF-κB expression in the positive control group. NF-κB activation also promotes NLRP3 inflammatory activation. Because IL-18 is an NLRP-3-related cytokine, its expression in the positive control group was also confirmed to be increased [7]. The experimental data showed that GTE decreased the inflammation marker (Figure 1-5) in the LPS-induced ARDS rats. This finding was supported by other studies in which the primary component of green tea, epigallocatechin-3-gallate (EGCG), was shown to have anti-inflammatory properties [11]. Black tea and green tea both have an anti-inflammatory action that prevents the denaturation of proteins [39]. Green tea reduces the activity of NF-κB by acting as an antioxidant to scavenge ROS [11,14]. Phytochemical assay of green tea showed very high phenol (++++) and flavonoid (++++) contents. Green tea contains catechin equivalent to 23.33 µg/mg extract [40]. Green tea leaves contain catechins (such as epigallocatechin-3-gallate (EGCG), quercetin, thearubigins, chlorogenic acid, caffeine, theaflavins, theanine, and gallic acid) [41]. Green tea has high antioxidant properties toward 2,2-diphenyl-1-picrylhydrazyl (DPPH) free radical scavenging with IC_{50} of 0.487 µg/mL [40], and 24.00 µg/mL [14]. TNF-α, IL-1β, and MMPs, as well as other genes and proteins linked to inflammation, are affected by green tea and its catechins. [11]. Green tea enhances cell viability significantly, decreasing IL-6, IL-1β, and TNF-α gene expression contrasted with LPS-treated HGEK cells as inflammation model [42]. Green tea and its catechins affect inflammatory responses downstream of NF-κB activation [43]. By reducing the NF-kB-mediated inflammatory response, GTE is able to both directly scavenge ROS and indirectly decrease ROS generation [43]. The principal element in green tea, EGCG, possesses anti-inflammatory and protective characteristics against oxidative damage [44]. Other studies have found that antioxidant compounds can block the activation of NLRP3 inflammation and the increased secretion of proinflammatory cytokines like IL-18 and IL-1. This supports the notion that ROS are involved in the NLRP3 inflammatory pathway [45]. EGCG reduces pro-inflammatory expression mediators, including inducible nitric oxide (iNOS), TNF-α, IL-1β, and IL-6, in the LPS induced acute lung injury (ALI) [44]. EGCG, the major compound of green tea, suppresses production of cyclooxigenase-2 (COX-2), NO, IL-1β, IL-6, TNF-α in macrophage cells stimulated by LPS [10]. In human chondrocytes induced by LPS and murine macrophages induced by LPS, EGCG inhibits the expression of iNOS via preventing NF-kB activation [46]. The major component of GTE, EGCG, significantly decreased TRIF, MyD88, TLR-4, and p-p65 in the lung tissue of LPS-induced male BALB/C mice as ALI model. It also significantly lowers IL-1β, TNF-α, and IL-6 in the blood, lungs, and fluid from the bronchoalveolar lavage [47].

4   Conclusion

In conclusion, this study showed the potential of GTE in reducing LPS-induced cytokine levels, indicated by decreasing serum IL-18 levels; lung TNF-α; IL-12 levels; IL-6 protein expression; NF-κB; NLRP-3 gene expression; bleeding score; inflammation score; and alveolar collapse score of lung damage after GTE treatment.

5   Acknowledgments

References

[1]   Acosta, M.A.T. & Singer, B.D.*, Pathogenesis of COVID-19-Induced ARDS: Implications for an Ageing Population*, European Respiratory Journal, **56**(3), pp. 2002049, 2020.

[2]   Azmi, N.U., Puteri, M.U. & Lukmanto, D., *Cytokine Storm in COVID-19: An Overview, Mechanism, Treatment Strategies, and Stem Cell Therapy Perspective*, Pharmaceutical Sciences and Research, **7**(4), pp. 1-11, 2020.

[3]   Ye, Z., Zhang, Y., Wang, Y., Huang, Z. & Song, B., *Chest CT Manifestations of New Coronavirus Disease 2019 (COVID-19): A Pictorial Review*, European Radiology, **30**, pp. 4381-4389, 2020.

[4]   Minciullo, P.L, Catalano, A., Mandraffino, G., Casciaro, M., Crucitti, A., Maltese, G., Morabito, N., Lasco, A., Gangemi, S. & Basile, G., *Inflammaging and Anti-Inflammaging: The Role of Cytokines in Extreme Longevity*, Archivum Immunologiae et Therapiae Experimentalis (Warsz), **64**, pp. 111-126, 2016.

[5]   Zhou, Y., Hong, Y. & Huang, H., *Triptolide Attenuates Inflammatory Response in Membranous Glomerulo-Nephritis Rat via Downregulation of NF-κB Signaling Pathway*, Kidney and Blood Pressure Research, **41**(6), pp. 901-910, 2016.

[6]   Freeman, T.L. & Swartz, T.H., *Targeting the NLRP3 Inflammasome in Severe COVID-19*, Frontiers in Immunology, **11**, pp. 1518, 2020.

[7]   Qu, J., Wang, W., Zhang, Q. & Li, S., *Inhibition of Lipopolysaccharide-Induced Inflammation of Chicken Liver Tissue by Selenomethionine via*

TLR4-NF-κB-NLRP3 Signaling Pathway, Biological Trace Element Research, **195**, pp. 205-214, 2020.

[8]   Ware, L.B., *Physiological and Biological Heterogeneity in COVID-19-Associated Acute Respiratory Distress Syndrome*, The Lancet Respiratory Medicine, **8**(12), pp. 1163-1165, 2020.

[9]   Shrestha, G.S., Khanal, S., Sharma, S. & Nepal G., *COVID-19: Current Understanding of Pathophysiology*, Journal of Nepal Health Research Council, **18**(3), pp. 351-359, 2020.

[10]   Novilla, A., Djamhuri, D.S., Nurhayati, B., Rihibiha, D.D., Afifah, E. & Widowati, W., *Anti-Inflammatory Properties of Oolong Tea (Camellia Sinensis) Ethanol Extract and Epigallocatechin Gallate in LPS-induced RAW 264.7 Cells*, Asian Pacific Journal of Tropical Biomedicine, **7**(11), pp. 1005-1009, 2017.

[11]   Ohishi, T., Goto, S., Monira, P., Isemura, M. & Nakamura, Y., *Anti-Inflammatory Action of Green Tea*, Allergy Agents in Medicinal Chemistry, **15**(2), pp. 74-90, 2016.

[12]   Mazgaeen, L. & Gurung, P., *Recent Advances in Lipopolysaccharide Recognition Systems*, International Journal of Molecular Sciences, **21**(2), pp. 1-18, 2020.

[13]   Domscheit, H., Hegeman, M.A., Carvalho, N. & Spieth, P.M., *Molecular Dynamics of Lipopolysaccharide-induced Lung Injury in Rodents*, Frontiers in Physiology, **11**(36), pp. 1-8, 2020.

[14]   Priyandoko, D., Widowati, W., Kusuma, H.S.W., Afifah, E., Wijayanti, C.R., Wahyuni, C.D., Idris, A.M., Putdayanti, R.A. & Rizal, R., *Antioxidant Activity of Green Tea Extract and Myricetin*, in 2021 IEEE International Conference on Health, Instrumentation & Measurement, and Natural Sciences (InHeNce), IEEE, **2021**(2021), pp. 1-5, 2021.

[15]   Zhang, S., Wang, P., Zhao, P., Wang, D., Zhang, Y., Wang, J., Chen, L., Guo, W., Gao, H. & Jiao, Y., *Pretreatment of Ferulic Acid Attenuates Inflammation and Oxidative Stress in a Rat Model of Lipopolysaccharide-Induced Acute Respiratory Distress Syndrome*, International Journal of Immunopathology and Pharmacology, **31**, pp. 394632017750518, 2018.

[16]   Mokhtari-Zaer, A., Norouri F., Askari, V.R., Khadzair, M.R., Roshan, N.M., Boskabady M., Hosseini M. & Boskabady M.H., *The Protective Effect of Nigella Sativa Extract on Lung Inflammation and Oxidative Stress Induced by Lipopolysaccharide in Rats*, Journal of Ethnopharmacology, **253**, pp. 112653, 2020.

[17]   Wahby, M.M., Yacout, G., Kandeel, K. & Awad D., *LPS-Induced Oxidative Inflammation and Hyperlipidemia in Male Rats: The Protective Role of Origanum Majorana Extract*, Beni-Suef University Journal of Basic and Applied Sciences, **4**(4), pp. 291-298, 2015.

[18]   Widowati, W., Wargasetia, T.L., Rahardja, F., Gunanegara, R.F., Priyandoko, D., Gondokesumo, M.E., Novianto, A., Yati, A. & Rizal, R.,

Human Wharton's Jelly Mesenchymal Stem Cells Inhibit Cytokine Storm in Acute Respiratory Distress Syndrome in a Rat Model, Asian Pacific Journal of Tropical Biomedicine, **12**(8), pp. 343-350, 2022.

[19] Priyandoko, D., Widowati, W., Afifah, E., Sholihah, I.A., Wahyuni, C.D., Wijayanti, C.R. & Rizal, R., *Soybean Seeds (Glycine Max L.) Extract Against Cytokine Storm in ARDS Rat Model Through Inhibiting Inflammation Marker*, Hayati, **30**(4), pp. 779-788, 2023.

[20] Widowati, W., Wargasetia, T.L., Rahardja, F., Gunanegara, R.F., Priyandoko, D., Gondokesumo, M.E., Novianto, A., Yati, A. & Rizal, R., *hWJMSCs Inhibit Inflammation and Apoptosis in an ARDS Cell Model.* Journal of Taibah University Medical Sciences, **18**(6), pp.1519-1526, 2023.

[21] Widowati, W., Afifah, E., Mozef T., Sandra, F., Rizal, R., Amalia, A., Arinta, Y., Bachtiar, I. & Murti, H., *Effects of Insulin-like Growth Factor-Induced Wharton Jelly Mesenchymal Stem Cells toward Chondrogenesis in an Osteoarthritis Model*, Iranian Journal of Basic Medical Sciences, **21**(7), pp. 745-752, 2018.

[22] Widowati, W., Jasaputra, D.K., Sumitro, S.B., Widodo, M.A., Afifah, E., Rizal, R., Kusuma, H.S.W., Murti, H., Bachtiar, I. & Faried, A., *Direct and Indirect Effect of TNFα and IFNγ Toward Apoptosis in Breast Cancer Cells*, Molecular and Cellular Biomedical Sciences, **2**(2), pp. 60-69, 2018.

[23] Gondokesumo, M.E., Pardianto, B., Handono K., Sumitro S.B., Widowati, W., Wismandanu, O., Hartady, T., Rosdianto, A.M., Goenawan, H., Lesmana R., Wathoni, N. & Supratman, U., *Garcinia Mangostana Extract Enhances Skin Epithelialization in Rat Induced Burn Injury*, Pakistan Veterinary Journal, **39**(3), pp. 365-370, 2019.

[24] Pham, N.A., Morrison, A., Schwock, J., Aviel-Ronen, S., Lakolev, V., Tsao, M.S., Ho, J. & Hedley, D.W, *Quantitative Image Analysis of Immunohistochemical Stains Using a CMYK Color Model*, Diagnostic Pathology, **2**(1), pp. 1-10, 2007.

[25] Ponti, G., Losi, L., Gregorio, C.D., Roncucci, L., Pedroni, M., Scarselli, A., Benatti, P., Seidenari, S., Pellacani, G., Lembo, L., Rossi, G., Marino, M., Lucci-Cordisco, E. & de Leon, M.P. ., *Identification of Muir-Torre Syndrome Among Patients with Sebaceous Tumors and Keratoacanthomas: Role of Clinical Features, Microsatellite Instability, and Immunohistochemistry*, Cancer, **103**(5), pp. 1018-1025, 2005.

[26] Lister, I.N.E., Ginting, C.N., Girsang, E., Nataya, E.D., Azizah, A.M. & Widowati, W., *Hepatoprotective Properties of Red Betel (Piper Crocatum Ruiz and Pav) Leaves Extract Towards H2O2-induced Hepg2 Cells via Anti-Inflammatory, Antinecrotic, Antioxidant Potency*, Saudi Pharmaceutical Journal, **28**(10), pp. 1182-1189, 2020.

[27] Ruiz-Villalba, A., Ruijter, J.M. & van den Hoff, M.J.B., *Use and Misuse of Cq in qPCR Data Analysis and Reporting,* Life, **11**(6), pp. 496, 2021.

[28] Fiala, A., Slagle, C., Legband, N., Aghabaglou, F. & Buesing, K., Borden, M., Harris, S. & Terry B., *Treatment of a Rat Model of LPS-Induced ARDS via Peritoneal Perfusion of Oxygen Microbubbles*, Journal of Surgical Research, **246**, pp. 450-456, 2020.

[29] Liu, G., Di, Z., Hao, C., Wang, W., Pei, T., Zheng, L., Long, H., Wang, H., Liao, W., Wang, W., Zhang, C., Li, X., Mi, Y., Yan, F. & Liu, Y., *Effects of Different Concentrations of Mesenchymal Stem Cells Treatment on LPS-Induced Acute Respiratory Distress Syndrome Rat Model*, Experimental Lung Research, **47**(5), pp. 226-238, 2021.

[30] Geng, C., Guo, Y., Wang, C., Cui, C., Han, W., Lia, D. & Jiang, P., *Comprehensive Evaluation of Lipopolysaccharide-induced Changes in Rats Based on Metabolomics*, Journal of Inflammation Research, **13**, pp. 477-486, 2020.

[31] Gu, T., Zhao, S., Jin, G., Song M., Zhi, Y., Zhao, R., Ma, F., Zheng, Y.,Wang, K., Liu, H., Xin, M., Han, W., Li, X., Dong, C. D., Liu, K. & Dong, Z., *Molecular Mechanism of SARS-Cov-2 Components Caused ARDS in Murine Model*, bioRxiv, pp. 1-25, 2020.

[32] Kircheis, R., Haasbach, E., Lueftenegger, D., Heyken, W.T., Ocker, M. & Planz, O., *NF-κB Pathway as a Potential Target for Treatment of Critical Stage COVID-19 Patients*, Frontiers in Immunology, **11**, pp. 1-11, 2020.

[33] Hirano, T. & Murakami, M., *COVID-19: A New Virus, but a Familiar Receptor and Cytokine Release Syndrome*, Immunity, **52**(5), pp. 731-733, 2020.

[34] Freeman, T.L. & Swartz, T.H., *Targeting the NLRP3 Inflammasome in Severe COVID-19*, Frontiers in Immunology, **11**, pp. 1-12, 2020.

[35] Shoemaker, W.C., Appel, P., Czer, L.S., Bland, R., Schwartz, S., & Hopkins, J.A., *Pathogenesis of ARDS Post Hemorrhage and Trauma*, Critical Care Medicine, **8**(9), pp. 504-512, 1980.

[36] Del Sorbo, L., Tonetti, T. & Ranieri, V.M., *Alveolar Recruitment in Acute Respiratory Distress Syndrome: Should We Open the Lung (No Matter What) or May Accept (Part of) the Lung Closed?*, Intensive Care Medicine, **45**(10), pp. 1436-1439, 2019.

[37] Cardinal-Fernandez, P., Lorente, J.A., Ballen-Barragan, A. & Matute-Bello, G., *Acute Respiratory Distress Syndrome and Diffuse Alveolar Damage New Insights on a Complex Relationship*, Annals of the American Thoracic Society, **14**(6), pp. 844-850, 2017.

[38] Nieman, G.F., Andrews, P., Satalin, J., Wilcox, K., Kollisch-Singule, M., Madden, M., Aiash, H., Nlair, S.J., Gatto, L.A. & Hamabshi, N.M, *Acute Lung Injury: How to Stabilize a Broken Lung*, Critical Care, **22**(136), pp. 1-11, 2018.

[39] Chatterjee, P., Chandra, S., Dey, P. & Bhattacharya, S., *Evaluation of Anti-Inflammatory Effects of Green Tea and Black Tea: A Comparative in Vitro*

Study, Journal of Advanced Pharmaceutical Technology and Research, **3**(2), pp. 136-138, 2012.

[40] Widowati, W., Herlina, T., Ratnawati, H., Constantia, G., Deva, I.D.G. S. & Maesaroh, M., *Antioxidant Potential of Black, Green and Oolong Tea Methanol Extracts*, Biology, Medicine, & Natural Product Chemistry, **4**(2), pp. 35-39, 2015.

[41] Bagheri, R., Rashidlamir, A., Ashtaru-Larky, D., Wong, A., Alipour, M., Motevalli, M.S., Chebbi, A., Laher, I. & Zouhal, H., *Does Green Tea Extract Enhance the Anti-Inflammatory Effects of Exercise on Fat Loss?*, British Journal of Clinical Pharmacology, **86**(4), pp. 753-762, 2020.

[42] Hagiu, A., Attin, T., Schmidlin, P.R. & Ramenzoni, L.L., *Dose-Dependent Green Tea Effect on Decrease of Inflammation in Human Oral Gingival Epithelial Keratinocytes: in Vitro Study*, Clinical Oral Investigations, **24**, pp. 2375-2383, 2020.

[43] Hodges, J.K., Sasaki, G.Y. & Bruno, R.S., *Anti-Inflammatory Activities of Green Tea Catechins Along the Gut–Liver Axis in Nonalcoholic Fatty Liver Disease: Lessons Learned from Preclinical and Human Studies*, Journal of Nutritional Biochemistry, **85**, pp. 108478, 2020.

[44] Almatroodi, S.A., Almatroudi, A., Anwar, S., Yousif, B.A., Khan, A.A., Alsahli, M.A. & Rahmani, A.H., *Antioxidant, Anti-Inflammatory and Hepatoprotective Effects of Olive Fruit Pulp Extract: in Vivo and In Vitro Study*, Journal of Taibah University for Science, **14**(1), pp. 1660-1670, 2020.

[45] Choe, J.Y. & Kim S.K., *Quercetin and Ascorbic Acid Suppress Fructose-Induced NLRP3 Inflammasome Activation by Blocking Intracellular Shuttling of TXNIP in Human Macrophage Cell Lines*, Inflammation, **40**, pp. 980-994, 2017.

[46] Ahn, H.Y. & Kim, C.H., *Epigallocatechin-3-Gallate Regulates Inducible Nitric Oxide Synthase Expression in Human Umbilical Vein Endothelial Cells*, Laboratory Animal Research, **27**(2), pp. 85-90, 2011.

[47] Wang, J., Fan, S.M. & Zhang, J., *Epigallocatechin-3-Gallate Ameliorates Lipopolysaccharide-Induced Acute Lung Injury by Suppression of TLR4/NF-kb Signaling Activation*, Brazilian Journal of Medical and Biological Research, **52**, pp. 1-7, 2019.